Bone Remodeling Following Mandibular Reconstruction using Fibula Free Flap

Keke Zheng[1], Nobuhiro Yoda[2], Junning Chen[3,4], Zhipeng Liao[1], Jingxiao Zhong[1], Chi Wu[1], Boyang Wan[1], Shigeto Koyama[5], Keiichi Sasaki[2], Christopher Peck[6], Michael Swain[1], and Qing Li[1].

[1] School of Aerospace, Mechanical and Mechatronic Engineering, The University of Sydney, NSW 2006, Australia

[2] Division of Advanced Prosthetic Dentistry, Tohoku University Graduate School of Dentistry, 4-1, Seiryo-machi, Aoba-ku, Sendai, Miyagi, 9808575, Japan

[3] College of Engineering, Mathematics, and Physical Sciences, University of Exeter, EX4 4QF United Kingdom

[5] Maxillofacial Prosthetics Clinic, Tohoku University Hospital, 1-1, Seiryo-machi, Aoba-ku, Sendai, Miyagi, 9808575, Japan

[6] Faculty of Dentistry, The University of Sydney, Sydney, NSW, 2006, Australia

*Correspondence to: Qing Li

Room S542, Mechanical Engineering Building (J07),

Darlington Campus, The University of Sydney, NSW 2006, Australia

Phone: +61-02 9351 8607; Fax: +61-02 9351 7060;

Email: qing.li@sydney.edu.au

Word count: 3486

Abstract

To investigate bone remodelling responses to mandibulectomy, a joint external and internal remodelling algorithm is developed here by incorporating patient-specific longitudinal data. The primary aim of this study is to simulate bone remodelling activity in the conjunction region with a fibula free flap (FFF) reconstruction by correlating with a 28-month clinical follow-up. The secondary goal of this study is to compare the long-term outcomes of different designs of fixation plate with specific screw positioning. The results indicated that the overall bone density decreased over time, except for the Docking Site (namely DS1, a region of interest in mandibular symphysis with the conjunction of the bone union), in which the decrease of bone density ceased later and was followed by bone apposition. A negligible influence on bone remodeling outcome was found for different screw positioning. This study is believed to be the first of its kind for computationally simulating the bone turn-over process after FFF maxillofacial reconstruction by correlating with patient-specific follow-up.

Keywords: Bone remodelling, Maxillofacial reconstruction, Placement design of fixation plate, Time-dependent remodelling algorithm. Clinical follow-up

1. Introduction

A large number of mandibular bone defects coupled with the loss of muscular and soft tissue attachments due to trauma, atrophy, or following ablation for tumors, potentially generate several significant problems, such as facial disfigurement, malocclusion and impaired oral function. Free vascularized tissue grafting has become a well-established clinical procedure and is now widely used for managing post-ablative defects to overcome such problems (Gbara et al., 2007; Hakim et al., 2015). Of various surgical options with free vascularized tissues available, fibula free flap (FFF) grafting has demonstrated fairly high reliability and adaptability for the reconstruction of substantial mandibular defects, due to its adequate length for even subtotal mandibular reconstruction and long vascular pedicle (Hidalgo, 1989; Hidalgo and Pusic, 2002; Hidalgo and Rekow, 1995). Despite these proven benefits, loss of several masticatory muscles due to resection can still cause unbalanced jaw movement and abnormal mastication, resulting in significant biomechanical changes over time (Narra et al., 2014; Wong et al., 2010). Thus, the mechanobiological responses for a reconstructed jaw may be largely altered, and would in-turn affect subsequent bone healing and remodeling activities (Frost, 1993; Zheng et al., 2019a). In our previous clinical study (Yoda et al., 2018), the morphological changes in the conjunction region of the host mandible and FFF were investigated. However, evaluation of longitudinal density change due to bone remodeling at each conjunction region of bone union, especially apposition and resorption process within the reconstructed structure, remains an open research question.

CT-based three-dimensional (3D) finite element (FE) models have exhibited compelling advantages in biomechanical analysis by precisely capturing anatomical features of an individual subject in a time-dependent fashion. This technique has been widely applied in orthopedic and prosthodontic research to assess, predict and manage bone adaptation processes as a result of various clinical interventions (Chen et al., 2015; Lin et al., 2010a). In maxillofacial reconstruction, for example, several studies have assessed the biomechanical roles of a fixation plate on the bridging/supporting reconstruction process (Knoll et al., 2006; Narra et al., 2014; Schuller-Götzburg et al., 2009), where stability of the whole system could have significant contribution on long term survival rate and clinical success. In this regard, Knoll et al. (2006) and Narra et al. (2014) explored different plate shapes, while Schuller et al. (2009) investigated the effects of different plate materials. Unfortunately, there has been no specific study on either the associated mandibular bone remodeling biomechanics or the role of the number and position of screws. With a proper bone remodelling algorithm, the effects of fixation plate can be assessed in a predictive way, thereby providing a means to optimizing placement of the fixation plate for long-term promotion of bone reunion and apposition.

A better understanding of mechanobiological responses and associated bone remodelling at the bone union regions can provide fundamental data for enhancing orofacial reconstruction outcomes. Therefore, this study aims to (1) investigate the time-dependent bone remodelling activity around the conjunction regions by correlating with patient-specific clinical follow-ups; and (2) assess the long-term effects of fixation plate and screwing placement on clinical outcomes. The methodological procedure developed and the results obtained are anticipated to provide some important insights into surgical planning for mandibular reconstruction.

2. Materials and Methods

2.1 Clinical acquisition

In this study, a 66-year-old male patient who underwent mandibular reconstruction for the tumor removal with osteotomized FFF was selected. A universal titanium fixation plate (Synthes, Solothurn, Switzerland), which was pre-bent based upon a CT-based 3D patient model prior to surgery and fixed monocortical with 11 titanium screws (Synthes, Solothurn, Switzerland). Multi-detector helical follow-up CT scans were performed at 4, 16, and 28 months after surgery (namely, M4, M16, and M28, respectively).

In this study, 18 volumes of interest (VOIs) of 2 mm^3 each were considered for two purposes: (1) as the reference to correlate the simulated remodeling results with clinical follow-up data; (2) as the region of interest to analyze long-term bone remodeling outcomes. To define the VOI, six planes parallel to the mandibular plane were selected at three docking sites (DS1, DS2, and DS3, Fig. 1a) with 2 mm intervals by multiple planar reconstructions (MPR). On each plane, the VOI was defined with a 2 mm area on each plane along the superior-inferior axis (Fig. 1b). The VOIs were created as a cube of the same size and placed in the constructed bone model (Fig. 2c). The fixation screws were modeled in Solidworks 2013 (SolidWorks Corp, Waltham, MA, USA) closely following the manufacture's specifications.

2.2 Finite element modeling

Three surface models were created for this specific patient based upon the CT scans at three dedicated time points (M4, M16, and M28) by using ScanIP Ver. 4.3 (Simpleware Ltd, Exeter, UK) for segmentation; and Rhinoceros 4.0 (Robert McNeel & Associates, Seattle, USA) for parametrization of the reconstructed 3D models in terms of non-uniform rational B-spline (NURBS) function. Our previous clinical study on this specific subject found that the morphological bone surface changes almost ceased from M16-M28. We then assume that the combination of the surface models at all these three-time points defines the surface boundary that the bone could potentially grow to the maximum for this patient. Therefore, a “resultant” model was obtained by merging all three surface models. This is because leaving extra room in the jaw model for assigning very low Young's modulus allows accomodating the potential growth of bone surface during remodelling. In order to achieve this, a CT pixel-based mapping algorithm (Field et al., 2010) was adopted to create the heterogeneous bone density distribution at time point M4, specifying initial bone morphology and extra space with a relatively low Young's modulus. All other material properties used in this study were summarized in Table 1.

Hinge constraints were prescribed for the corresponding mandibular condyles (Narra et al., 2014). In this subject, the extensive bone resection was accompanied by functional loss of the right masseter, medial pterygoid and temporalis muscles; consequently, masticatory conditions changed dramatically post-surgery. The magnitudes and directions of individual muscle forces were derived in our previous study (Zheng et al., 2019a) (Fig. 2a).

Four additional models were generated by rearranging the number and position of fixation screws, along with different screwing configurations (Fig. 2c). The final assemblies were exported to ABAQUS 6.13.1 (Dassault Systèmes, Tokyo, Japan) for the FE analysis (Fig. 2b). The implant components, including plate and screws, were assumed to be perfectly bonded with the bone for simplification, as the bone remodeling process simulated in this study started from month 4 after sugery when full osseointegration has been established (Yoda et al., 2018, Ferguson et al. 2021). This assumption would not take substantial effects on the regions where the surface bone remodeling is a main concern in this present study.

2.3 Bone remodeling algorithm

The FE-based bone remodeling simulation is based upon the Wolff’s law, where four phases of bone remodelling activities, namely underloading resorption, equilibrium (lazy zone), apposition (Frost, 1987; Huiskes et al., 1987), and overloading resorption (Crupi et al., 2004;

Oosterwyck et al., 2002, Li et al., 2007), are considered in response to a different degrees of mechanical stimulus from the specific homeostatic level (Carter, 1987, 1984; Frost, 1993).

In literature, the strain energy density (SED) per unit apparent density has been widely accepted as an appropriate mechanical stimulus for jawbone remodeling (Lin et al., 2010a; Weinans et al., 1992). In general, the rate equation in terms of density increment ($\Delta\rho$) over a time interval (Δt) can be formulated as,

$$\Delta\rho = \begin{cases} C_{ap}[\Xi - K(1+s)]\Delta t - C_{or}[\Xi - K(1+s)]^2\Delta t; & if\ \Xi > K(1+s) \\ 0; & if\ \ K(1-s) \leq \Xi \leq K(1+s) \\ C_{ur}[\Xi - K(1-s)]\Delta t; & if\ \ \Xi < K(1-s) \end{cases} \tag{1}$$

where the reference stimulus is given as $K = 0.00036\ (J/g)$ (Lin et al., 2010b) and the width of lazy zone given as $2s = 0.2$ (Rungsiyakull et al., 2010). Ξ is the mechanical stimulus in terms of strain energy density (SED) divided by local apparent bone density. C_{ap}, C_{or} and C_{ur} are the rate constants for bone apposition, overloading resorption, and underloading resorption, respectively. All these rate constants were determined by using an inverse identification procedure through correlation with the image data acquired from the dedicated clinical follow-up in months 4 (after initial healing) to 28 over a two-year time span. Note that the identification of the remodelling parameters was based upon the first stage through our patient-specific longitudinal study in clinic. The remodeling algorithm and parrameters established in the first stage was then used to futher predict the outcome of the second stage (from 2 years to 4 years), which was considered critical (e.g. 4-year mid-term outcome) for the surgeons and patients . As a result, C_{ap}, C_{or} and C_{ur} were determined to be 20 month g/cm^5, 5000 month^3 g/cm^7 and 20 month g/cm^5, respectively, for this specific patient study.

The minimum and maximum densities of reconstructed bone were set to be 0.7 and 2.0 g/cm^3, respectively (Lin et al., 2010a). It should be noted that the density change evaluated in Eq. (1) allows updating the boundary surface in the region of interest (RoI) through gradually upgrading void elements to solid elements in the boundary/interface (or other way around), thereby moving the surface. Therefore, the algorithm integrates both internal remodeling (bone density) and surface remodeling (bone front).

The time step in this study represented one month. The remodeling was implemented through a FORTRAN subroutine in ABAQUS, where the bone material properties in each element are evaluated as per the user-defined constitutive models. Fig. 3 provides a flowchart to depict the unified bone remodeling procedure.

In order to quantify the remodeling algorithm defined in Eq. (1), a python script was developed to convert the user-defined variables into virtual CTs (Liao et al., 2017). In this case, the FE-based virtual CT images were generated from the simulated densities at M4, M16 and M28, respectively, in order to quantitatively match the longitudinal CT data obtained from the clinical follow-up. The discrepancy of mean grayscale values in these 18 VOIs were obtained from clinical CT and FE virtual CT using MATLAB (MathWorks, Inc., Massachusetts, USA).

In this study, Pearson correlation analysis in Graph-Pad Prism 7 (GraphPad Software, Inc. CA,USA), was performed to quantify the correlation between the FE and clinical data at different time steps. The root mean square error (RMSE) was also calculated to report the possible prediction error from the present bone remodeling algorithm in Graph-Pad Prism 7.

To calculate the variations in bone density and mechanical stimulus in the regions of interest more appropriately, their volume averages were calculated as:

$$\rho = \frac{1}{V}\int_V \rho dV \cong \frac{\sum_{e=1}^{n} \rho_e V_e}{\sum_{e=1}^{n} V_e} \quad (2)$$

$$\Xi = \frac{1}{V}\int_V \Xi dV \cong \frac{\sum_{e=1}^{n} \Xi_e V_e}{\sum_{e=1}^{n} V_e} \quad (3)$$

3. Results

3.1 Bone remodeling outcome

Fig. 4 shows the correlations between the clinical CT and FE virtual CT images at two time periods, in which the Pearson correlation coefficient r values were evaluated to be 0.743 and 0.771 for durations M4-M16 and M4-M28, respectively ($p < 0.001$). In line with the biostatistics text (Norman and Steiner, 2008), $r \geq 0.7$ indicates a strong linear correlation in biological studies. Note that it is very difficult (if not impossible) to achieve a perfect correlation ($r = 1$) in the present circumstance, due to the coupled effects between physiological variation and mechanical stimulus, in which biological/genetic factors such as systemic mineral homeostasis, can to a certain extent influence the correlation between the FE simulation and the clinical follow-up. The root mean square error (RMSE) of both correlation period M4-M16 and M4-M28 are calculated as 11.15 and 9.81, respectively, which indicating that the present bone remodeling algorithm might have a possible average error of 10.48% for bone change prediction .

Fig. 5 shows the simulated density distribution in the whole mandible and from each cross-sectional DS view. Four-time points were selected at M4, M16, M28, and M48 (predicted). In general, the bone density varies substantially from M4 to M16, but the variation is leveled off from M16. Commencing from the bone structure at M4, we also simulated the structural surface change together with internal bone remodeling. It is observed that in DS1, the growth of cortical region dilated from M4 to M16, but ceased from M16 onward. The bone apposition mainly occurred in the superior region of the bone, exhibiting formation of cortical bridging, which is considered as a predictor of establishing bone union strength (Akashi et al., 2015). In the cancellous region, on the other hand, decrease of density can be observed, suggesting the resorption in the inner region of the mandibular bone. In DS2, a similar trend of bone formation is observed, and bone apposition in the cortical region also occurred mainly on the superior surface. However, the decrease of bone density in the cancellous region is not as dramatic as in DS1. In DS3, the decrease of bone density is observed for both cortical and cancellous regions.

3.3 Effects of different screw positioning

Fig. 6 plots the longitudinal change of density at each DS for different screwing designs. For all the DSs, the overall density decreases in the course of bone remodeling. In DS1, the density rapidly reduced in the first 12 months and continues to decrease at a slower rate until month 33, followed by a density increase thereafter. These observations suggest that although the cortical bone region is expanding, the decrease of density in the cancellous bone progressed at a relatively faster rate, which dominated the overall density variation. Starting from month 33, resorption in the cancellous region halted, while the cortical bridge density kept increasing and resulted in increase of the overall density. In DS2, the overall bone density increased for the first 12 months and thereafter gradually decreased with time. For DS3, the density continued to decrease from M4 onward at almost a constant rate. This trend of density variation agrees with the change in density contour in Fig. 5b, where no much bone apposition was observed in DS3.

Concerning different designs of screwing number and position, Design 4, with the most screws installed, does have a relatively lower resorption rate for the first 12 months and a higher apposition rate from month 27 in DS1. In DS2, Design 1 with the least screws, had a faster bone resorption rate than the other designs with more screws. There is no significant difference with all these designs in DS3. While there are certain differences in bone remodeling outcomes with different fixation placements, the deviation is considered too small to draw a clinical recommendation from a remodeling prediction perspective.

4. Discussion

Note that the simulation of bone remodeling in this study started from month 4, as initial healing is known to generally take 6 to 12 weeks to a significant degree (Marsell and Einhorn, 2011). This stage acts substantially different from bone remodeling, and thereby cannot simply be interpreted and simulated by the current bone remodeling algorithm established (Calvo-Echenique et al., 2019; Isaksson et al., 2006). This study developed a joint remodeling procedure for accommodating morphological variation in both internal density and external shape of bony structure by following a topology optimization algorithm developed for engineering structures. Specifically, we placed some void regions by assigning a virtually low Young's modulus material, allowing to be gradually evolved into bony materials, thereby simulating surface growth of bone.

In this study, the simulated remodeling results respond to the functional load measured for this specific patient. During functional loading, the maximum stress is observed around region DS1 of the symphysis. Due to distortion induced by unilateral loading in the reconstructed mandible, the overall functional loading can be described as a combination of sagittal and transverse bending (Wong et al., 2010). As a result, the primary loading reaches the maximum in the middle plane of the mandible (i.e. DS1 in this case). In addition, the large difference in the cross-sections between the mandible and the fibula free flap in the DS1 region results in high-stress gradients in this area. Therefore, the overall mechanical stimulus (i.e. strain energy density per unit apparent density) in the symphysis region reaches a maximum and then gradually decreases upon approaching the end of the mandibular arch (i.e. towards the ramus area). As shown in Fig. 2b, higher SEDs were observed in both DS1 and DS2, compared to DS3. In other words, there was insufficient mechanical stimulation in DS3, thereby leading to bone resorption at a constant rate.

Since the mechanical stimulus is considered to be a trigger to initiate bone remodeling, high accumulation of SED on both DS1 and DS2 results in bone formation in the conjunction areas. Similar to the cortical bridging forming in DS1, bone apposition on the superior region of DS2 was also triggered by the high SED. However, in DS1, once the cortical bridge is established properly, the mechanical stimulus ceases increasing as less strain could develop in those regions, which to a certain extent, explains why the cortical region stops growing from M16 afterward. For the same reason, the mechanical stimulus decreased in the cancellous region, and such an under-loading condition casued bone resorption.

It is interesting to note that the inferior cortical region experienced bone resorption after M28 (Fig. 5b), while the superior aspect of cortical bone remains in equilibrium. The possible reason may be related to formation of a proper cortical bridge from M4 to M28, whereby the increasing strength on the superior surfaces enabled it to withstand more loads and consequently, less load was transferred to the inferior side. The associated reducation in mechanical stimulation appears to approach the lower thresholds of the effective SED, thereby triggering underloading bone resorption in the region.

The accumulation of stress in the DS1 region due to the altered functional loading in the reconstructed mandible also explains why bone resorption in DS1 can be reversed from 33 month post-surgery. The latter was followed by a gradual increase in overall bone density, in which the mechanical stimulus exceeded the upper threshold of the SED, thus changing from overall resorption to overall apposition. The bone apposition ceased once an equilibrium was reached, implying that the reduced mechanical stimulus falled into the lazy zone at this stage. In comparison, bone resorption in DS2 and DS3 continued over time as the relatively lower mechanical loading and stimuli were transferred to these areas. It is speculated that an implant-supported denture may be a possible solution that has been commonly considered as an option for functional rehabilitation following mandibular reconstruction (Hakim et al., 2015). This may lead to different biomechanical conditions and remodelling outcomes. Although the timing of such implant placement remains controversial, increasing biomechanical stimulation through the application of symmetrical functional loading might enable to better engage bony tissues in regions DS2 and DS3.

There are few studies in literature that have investigated the longitudinal bone variation for patients undergone mandibular reconstruction using fibula free flap. Disa et al. (1999) and Zoumalan et al. (2009) reported, on average, there are 10 and 20% bone height loss in the fibula free flaps following reconstruction, respectively. Disa et al. (1999) also investigated the different loss percentage of bone height for the patient with a 48 month follow-up in three specific regions: anterior (DS1), body (DS2), ramus areas (DS3), which are 5.8, 10 and 4.1%, respectively. In comparison, the predicted bone losses over the 48 months in the present study of these three regions are 4.2, 2.7 and 3.1%, respectively. To be noted, the both above literature studies suggested bone height loss by measuring the midportion of the region of interest on X-Ray scans; while in the our study, the bone loss percentage is measured by comparing the overall changes of bone volume in 3D space. This might explain why the overall bone loss in the present study is less than that reported in Disa et al.'s study (1999). Our results could have been more conservative as more remodeling information was captured. Moreover, in Disa et al's study (1999), the DS2 is substantially higher than the other two regions, which might be due to the fact that the inclined angle of DS2 to the image plane is likely to cause excessive X-ray scattering compared to the other two regions where DS1 and DS3 is more parallel and perpendicular to the image plane, respectively.

Fixation plates are commonly used to connect and support the grafted bone with the mandibular stumps. The role of the fixation plates is to stabilize the mechanical environment and transfer the loading to the transplant in a controllable manner. For this reason, the appropriate positioning of these screws is thought to be critically important surgically. Despite the different options of numbers and positioning of screws, they have one particular aspect in common, i.e. there are always two screws placed on each side of the conjunction region of bone union (i.e. DS1, DS2 and DS3), where the pairs of screws play a critical role in establishing substantial structural stability. This also explains why different designs led to marginal differences in bone remodeling outcomes in those regions. Design 4 has the most screw numbers, which does show a relatively slower bone resorption rate than the other designs (Fig. 6). For this reason, Design 4 has the highest the bone apposition rate in DS1 after month 33, and the lowest bone resorption rate in DS2 and DS3. It is believed that use of more screws does provide a more stable and stiffer system, in which the plate transfers more loading, thereby either slowing down bone loss or increasing bone formation in the union regions. Nevertheless, while this appears to an area of limited consequence for the present patient model, this could be a research question for further study on other patients.

Regarding application of the proposed unified time-dependent algorithm for estimating surface remodeling, it is still controversial in literature as some researchers have claimed external and internal bone remodeling exhibit different mechanisms (Carter, 1984; Weinans et al., 1992). Along with incorporating virtual soft (void) materials with a very low Young's modulus surrounding the cortical region, the simulated surface remodeling results exhibit a reasonable match with the clinical data acquired. It is noted that there exist certain discrepancies when matching the simulation with the clinical data, such as the superior region in DS3. The clinical complexity of such reconstructed regions (e.g. DS3) introduces some challenges for a comprehensive correlation between them. However, for a relatively less complicated region, such as DS2, the current remodeling algorithms provided a fairly realistic simulation. Regarding the density prediction in the region surrounding the VOIs, where the internal bone remodeling may have dominated bone turnover, the simulated results correlate better with the clinical follow-up.

Another limitation would be the patient-specific nature of this study. The remodeling algorithm, parameters and simulation results were based upon only one particular subject. Other patient factors, such as their systemic background, bone's conditions and surgical procedures, could be considered as additional decisive factors influencing the bone remodeling process. Further evaluation and data acquisition of other subjects with inevitably varied conditions are necessary before generalizing these clinical and biomechanical findings.

Regarding the possible evolution of remodelling parameters, it remains an open research question in literature. The remodelling parameters per se are patient-specific due to the fact that the physiological and biomechanical environments vary with ageing, health status, medication, and life-styles, etc. The interaction between physiological and mechanical conditions can be rather complex; so from our point of view, whether using evolving or constant remodeling parameters depends on the accepted level of correlation with clinical data. One of our previous studies did consider envoling remodeling parameters (Liao et al. 2017) at different remodeling stages. While such a method is more realistic in principle, we decided to use the constant remodeling coefficient as it is more efficient and easier to handle, given the bone remodeling results (i.e. correlation coefficient) derived from the both methods are quite indifferent.

5. Conclusion

In this patient-specific case study on the biomechanics of the orofacial reconstruction using fibula free flap (FFF), a time-dependent finite element (FE) based remodelling algorithm is developed by correlating longitudinal clinical data. A unified internal and external remodeling procedure was proposed here to investigate the bone's responses in three specific regions of bone union (namely DS1, DS2, DS3) over a four-year treatment period (up to 48 months). It is found that the overall bone density decreased over time, except for region DS1, where bone apposition started at 33 months after undergoing a certain period of resorption. A neglectable effect was observed for the different splint designs of screw numbers and positioning. In spite of the intrinsic limitations, this study is believed to be the first of its kind by developing a unified remodeling procedure for major orofacial reconstruction.

Acknowledgments

This work was supported by the Australian Research Council (ARC) (IC170100022 and DP180104200).

Conflict of interest

Authors have no conflict of interest concerning the present manuscript.

Table 1. Material properties adopted in FE models

Materials	Young's Modulus (MPa)	Poisson's ratio
Bone	Heterogeneous	0.30
Periodontal ligament (PDL)	Hyperelastic (Marlow)	0.45
Teeth (enamel and dentine)	20,000	0.20
Titanium (Implant, abutment, screw)	110,000	0.35

Figures

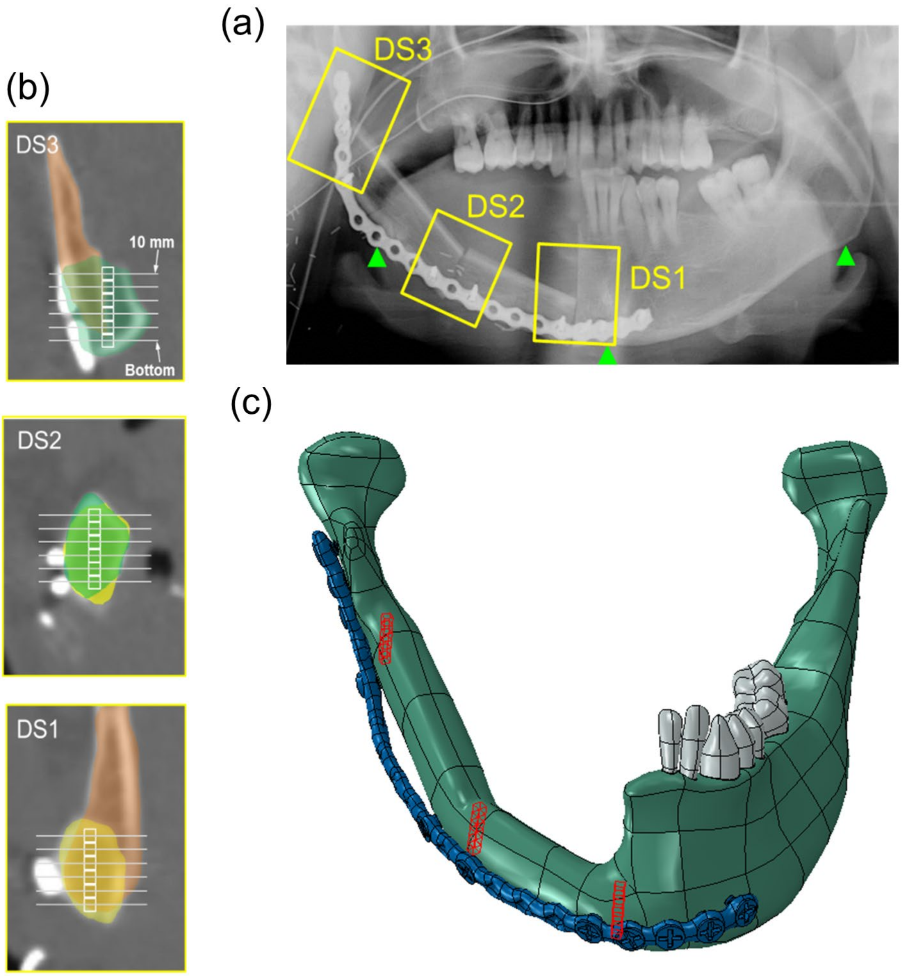

Fig. 1. Illustration of volume of interest (VOIs). (a) three investigated docking sites (DS1, DS2 and DS3) for the bone union; (b) VOIs placement in each docking site; and (c) VOIs definition in the 3D FE model.

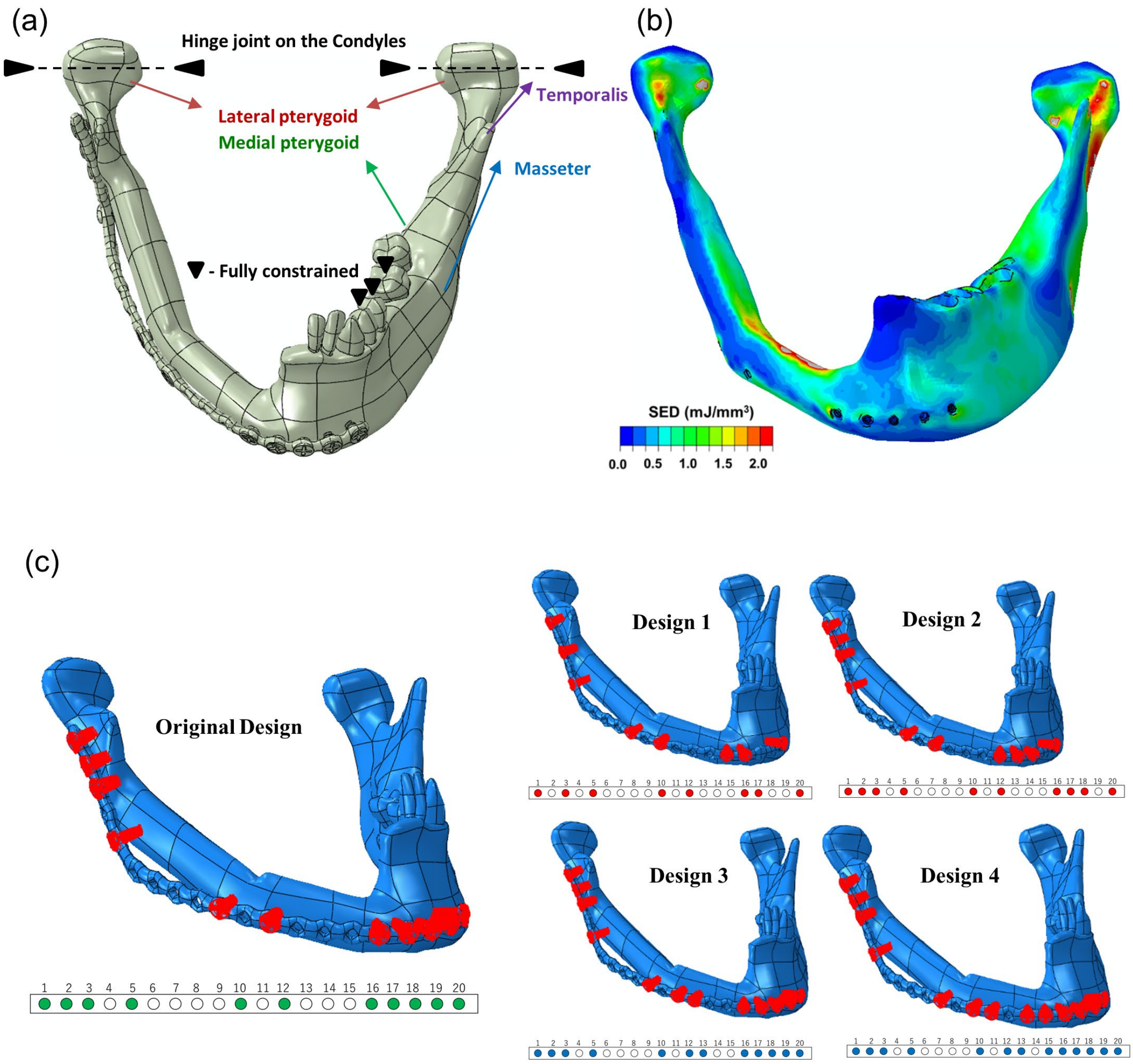

Fig. 2. The schematic of finite element modeling. (a) illustration of loading and boundary conditions applied; (b) Contour of strain energy density (SED) distribution simulated in the assembly; and (c) illustration of the plate – screwing configuration with different designs.

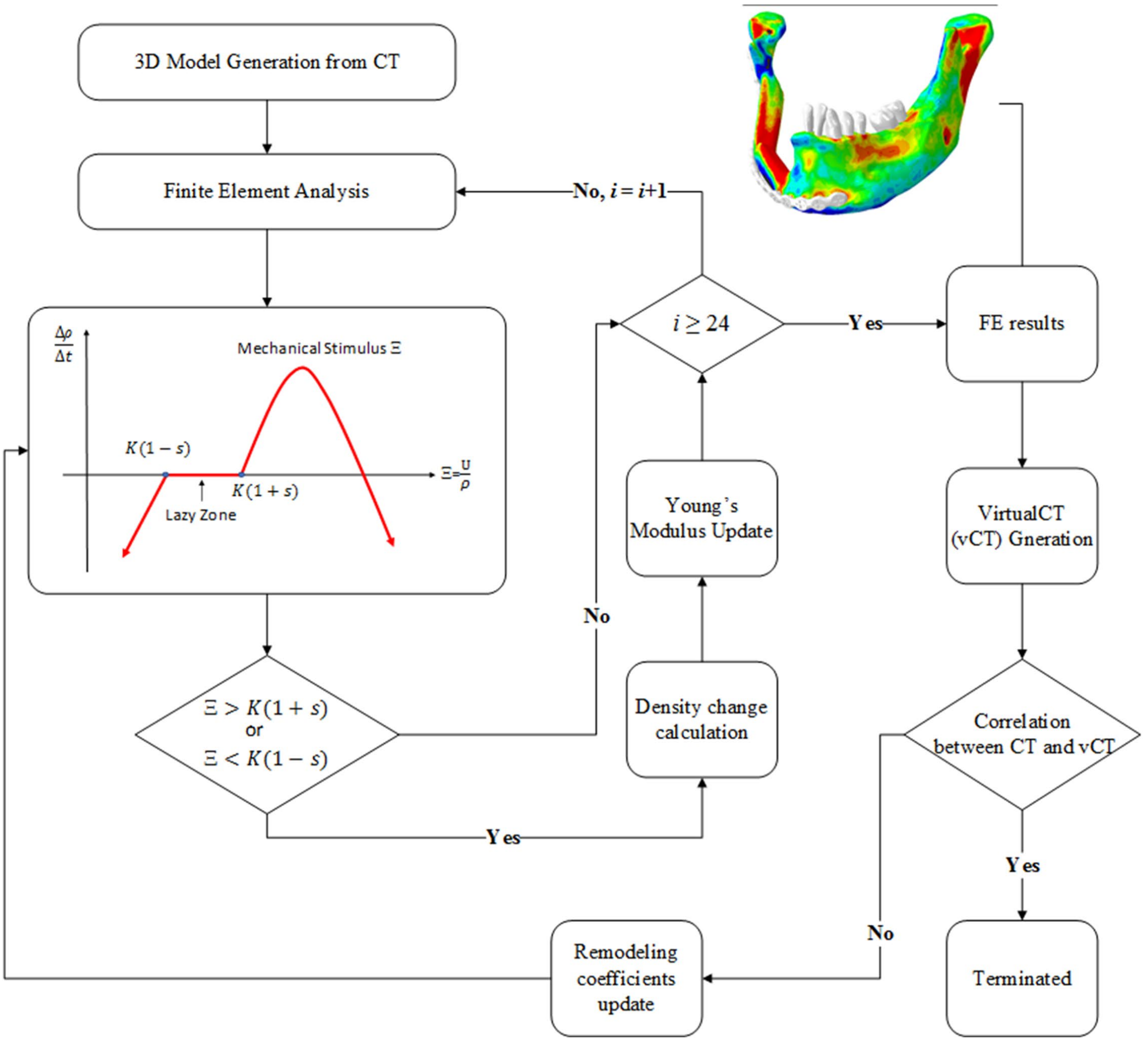

Fig. 3. Flowchart of the unified bone remodeling procedure for correlating with clinical follow-up data.

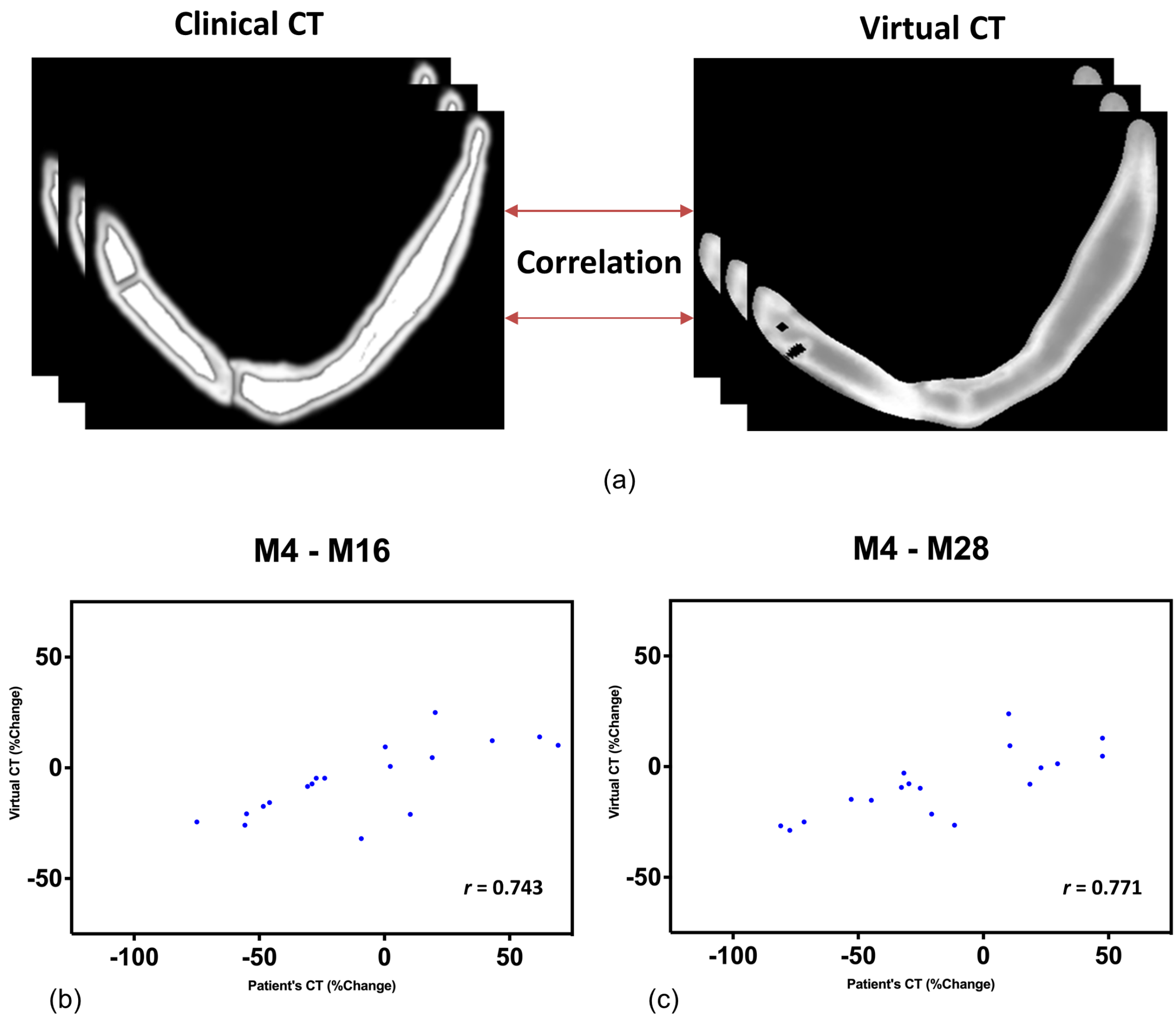

Fig. 4. (a) Demonstration of the correlation between clinical CT and virtual CT images. Pearson correlation analysis between the changes of VOI grayscale values in the clinical CT and FE virtual CT, for (b) M4 – M16 (Month 4 – Month 16) and (c) M4 -M28 (Month 4 – Month 28).

Fig. 5. Longitudinal changes of density from M4 to M48. (a) Overview of the density change on the whole mandible; and (b) cross-sectional images of the density variation in each DS.

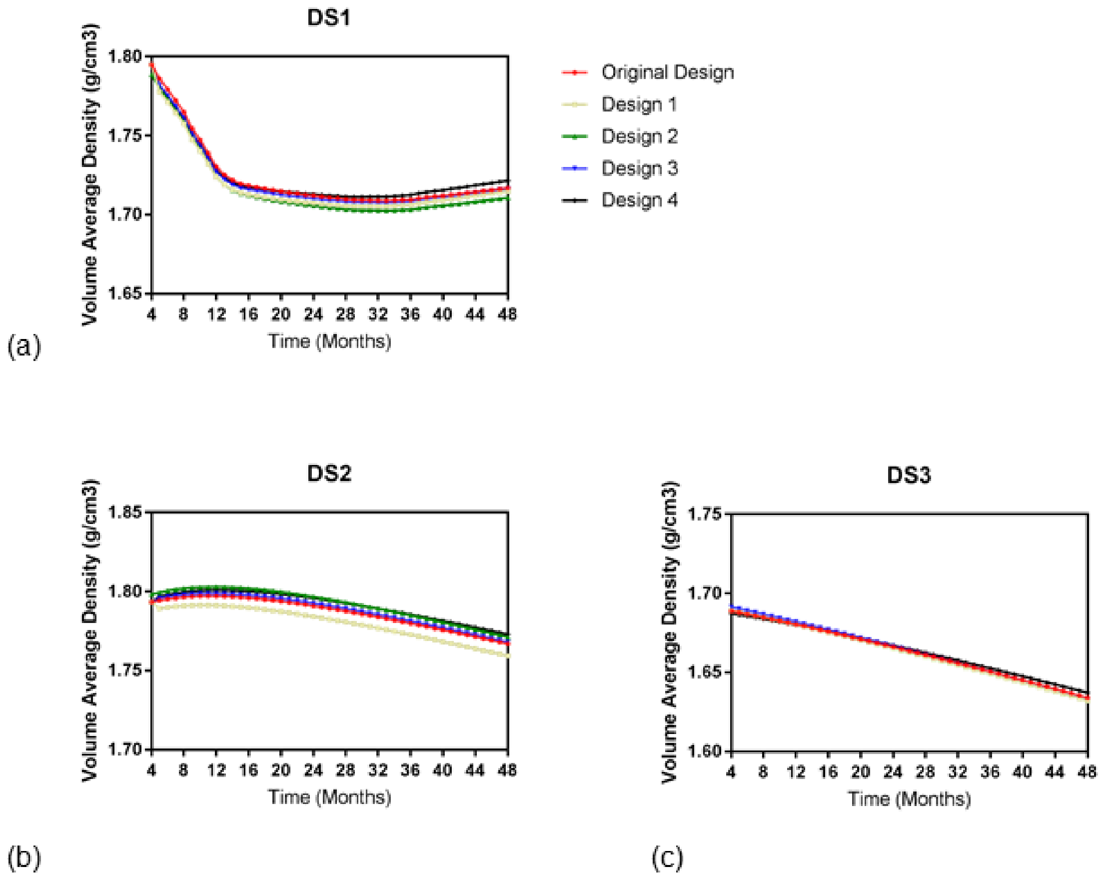

Fig. 6. Remodeling progresses in the regions of interest at (a) DS1, (b) DS2 and (b) DS3 region from 4 to 48 months.

References

Akashi, M., Hashikawa, K., Kakei, Y., Sakakibara, A., Hasegawa, T., Minamikawa, T., 2015. Sequential evaluation for bone union of transferred fibula flaps in reconstructed mandibles: Panoramic X-ray versus computed tomography. International Journal of Oral and Maxillofacial Surgery 44, 942–947. https://doi.org/ 10.1016/j.ijom.2015.04.014

Calvo-Echenique, A., Bashkuev, M., Reitmaier, S., Pérez-del Palomar, A., Schmidt, H., 2019. Numerical simulations of bone remodelling and formation following nucleotomy. Journal of Biomechanics 88, 138–147. https://doi.org/10.1016/j.jbiomech.2019.03.034

Carter, D.R., 1987. Mechanical loading history and skeletal biology. Journal of Biomechanics 20, 1095–1109. https://doi.org/10.1016/0021-9290(87)90027-3

Carter, D.R., 1984. Mechanical loading histories and cortical bone remodeling. Calcified Tissue International 36. https://doi.org/10.1007/BF02406129

Chen, J., Ahmad, R., Suenaga, H., Li, W., Swain, M., Li, Q., 2015. A comparative study on complete and implant retained denture treatments - A biomechanics perspective. Journal of Biomechanics 48, 512–519. https://doi.org/10.1016/j.jbiomech.2014.11.043

Chen, J., Li, W., Swain, M. v, Darendeliler, M.A., Li, Q., 2014. A periodontal ligament driven remodeling algorithm for orthodontic tooth movement. Journal of Biomechanics 47, 1689–1695. https://doi.org/10.1016/j.jbiomech.2014.02.030

Crupi, V., Guglielmino, E., la Rosa, G., vander Sloten, J., van Oosterwyck, H., 2004. Numerical analysis of bone adaptation around an oral implant due to overload stress. Proceedings of the Institution of Mechanical Engineers. Part H, Journal of engineering in medicine 218, 407–15. https://doi.org/10.1243/0954411042632171

Disa, J.J., Hidalgo, D.A., Cordeiro, P.G., Winters, R.M., Thaler, H., 1999. Evaluation of Bone

Height in Osseous Free Flap Mandible Reconstruction: An Indirect Measure of Bone Mass. Plastic & Reconstructive Surgery 103, 1371–1377. https://doi.org/10.1097/00006534-199904050-00005

Ferguson BM, Entezari A, Fang J, Li Q., 2021. Optimal placement of fixation system for scaffold-based mandibular reconstruction. Journal of the Mechanical Behavior of Biomedical Materials. https://doi.org/10.1016/j.jmbbm.2021.104855

Field, C., Li, Q., Li, W., Thompson, M., Swain, M., 2010. Prediction of mandibular bone remodelling induced by fixed partial dentures. Journal of Biomechanics 43, 1771–1779. https://doi.org/10.1016/j.jbiomech.2010.02.016

Frost, H.M., 1993. Wolf Law and bone’s structureal adaptations to mechanical usdage. The Angle Ortodontist.

Frost, H.M., 1987. Bone “mass” and the “mechanostat”: A proposal. The Anatomical Record 219, 1–9. https://doi.org/10.1002/ar.1092190104

Gbara, A., Darwich, K., Li, L., Schmelzle, R., Blake, F., 2007. Long-Term Results of Jaw Reconstruction With Microsurgical Fibula Grafts and Dental Implants. Journal of Oral and Maxillofacial Surgery 65, 1005–1009. https://doi.org/10.1016/j.joms.2006.06.294

Hakim, S.G., Kimmerle, H., Trenkle, T., Sieg, P., Jacobsen, H.C., 2015. Masticatory rehabilitation following upper and lower jaw reconstruction using vascularised free fibula flap and enossal implants—19 years of experience with a comprehensive concept. Clinical Oral Investigations 19, 525–534. https://doi.org/10.1007/s00784-014-1247-9

Hidalgo, D.A., 1989. Fibula free flap: A new method of mandible reconstruction. Plastic and Reconstructive Surgery 84, 71–79. https://doi.org/10.1097/00006534-198907000-00014

Hidalgo, D.A., Pusic, A.L., 2002. Free-flap mandibular reconstruction: a 10-year follow-up study. Plastic & Reconstructive Surgery 110, 431–438.

Hidalgo, D.A., Rekow, A., 1995. A review of 60 consecutive fibula free flap mandible reconstructions. Plastic and Reconstructive Surgery 96, 585–596. https://doi.org/10.1097/00006534-199509000-00010

Huiskes, R., Weinans, H., Grootenboer, H.J., Dalstra, M., Fudala, B., Slooff, T.J., 1987. Adaptive bone-remodeling theory applied to prosthetic-design analysis. Journal of Biomechanics 20, 1135–1150. https://doi.org/10.1016/0021-9290(87)90030-3

Isaksson, H., van Donkelaar, C.C., Huiskes, R., Ito, K., 2006. Corroboration of mechanoregulatory algorithms for tissue differentiation during fracture healing: comparison with in vivo results. Journal of Orthopaedic Research 24, 898–907. https://doi.org/10.1002/jor.20118

Knoll, W.D., Gaida, A., Maurer, P., 2006. Analysis of mechanical stress in reconstruction plates for bridging mandibular angle defects. Journal of Cranio-Maxillofacial Surgery 34, 201–209. https://doi.org/10.1016/j.jcms.2006.01.004

Li, J., Li, H., Shi, L., Fok, A.S.L., Ucer, C., Devlin, H., Horner, K., Silikas, N., 2007. A mathematical model for simulating the bone remodeling process under mechanical stimulus. Dental Materials 23, 1073–1078. https://doi.org/10.1016/j.dental.2006.10.004

Liao, Z., Yoda, N., Chen, J., Zheng, K., Sasaki, K., Swain, M.V., Li, Q., 2017. Simulation of multi-stage nonlinear bone remodeling induced by fixed partial dentures of different configurations: a comparative clinical and numerical study. Biomechanics and Modeling in Mechanobiology 16. https://doi.org/10.1007/s10237-016-0826-x

Lin, D., Li, Q., Li, W., Duckmanton, N., Swain, M., 2010a. Mandibular bone remodeling induced by dental implant. Journal of Biomechanics 43, 287–293. https://doi.org/10.1016/j.jbiomech.2009.08.024

Lin, D., Li, Q., Li, W., Swain, M., 2010b. Bone remodeling induced by dental implants of functionally graded materials. Journal of Biomedical Materials Research - Part B Applied Biomaterials 92, 430–438. https://doi.org/10.1002/jbm.b.31531

Marsell, R., Einhorn, T.A., 2011. The biology of fracture healing. Injury 42, 551–555. https://doi.org/10.1016/J.INJURY.2011.03.031

Narra, N., Valášek, J., Hannula, M., Marcián, P., Sándor, G.K., Hyttinen, J., Wolff, J., 2014. Finite element analysis of customized reconstruction plates for mandibular continuity defect therapy. Journal of Biomechanics 47, 264–268. https://doi.org/10.1016/j.jbiomech.2013.11.016

Norman, G.R., Steiner, D.L., 2008. Biostatistics: The Bare Essentials, PMPH USA.

Oosterwyck, H.V.A.N., Sloten, J. vander, Puers, R., Naert, I., 2002. Finite Element Studies on the Role of Mechanical Loading in Bone 441–451.

Rungsiyakull, C., Li, Q., Sun, G., Li, W., Swain, M. v., 2010. Surface morphology optimization for osseointegration of coated implants. Biomaterials 31, 7196–7204. https://doi.org/10.1016/j.biomaterials.2010.05.077

Schuller-Götzburg, P., Pleschberger, M., Rammerstorfer, F.G., Krenkel, C., 2009. 3D-FEM and histomorphology of mandibular reconstruction with the titanium functionally dynamic bridging plate. International Journal of Oral and Maxillofacial Surgery 38, 1298–1305. https://doi.org/10.1016/j.ijom.2009.07.060

Weinans, H., Huiskes, R., Grootenboer, H.J., 1992. The behavior of adaptive bone-remodeling simulation models. Journal of Biomechanics 25, 1425–1441. https://doi.org/10.1016/0021-9290(92)90056-7

Wong, R.C.W., Tideman, H., Kin, L., Merkx, M.A.W., 2010. Biomechanics of mandibular reconstruction: a review. International Journal of Oral and Maxillofacial Surgery. https://doi.org/10.1016/j.ijom.2009.11.003

Yoda, N., Zheng, K., Chen, J., Liao, Z., Koyama, S., Peck, C., Swain, M., Sasaki, K., Li, Q., 2018. Biomechanical analysis of bone remodeling following mandibular reconstruction using fibula free flap. Medical Engineering and Physics 56, 1–8. https://doi.org/10.1016/j.medengphy.2018.03.008

Zheng, K., Liao, Z., Yoda, N., Fang, J., Chen, J., Zhang, Z., Zhong, J., Peck, C., Sasaki, K., Swain, M. v., Li, Q., 2019a. Investigation on masticatory muscular functionality following oral reconstruction – An inverse identification approach. Journal of Biomechanics 90, 1–8. https://doi.org/10.1016/j.jbiomech.2019.04.007

Zoumalan, R.A., Hirsch, D.L., Levine, J.P., Saadeh, P.B., 2009. Plating in microvascular reconstruction of the mandible: Can fixation be too rigid? Journal of Craniofacial Surgery 20, 1451–1454. https://doi.org/10.1097/SCS.0b013e3181af156a